SCIENTIFIC PAPERS
OF THE UNIVERSITY OF PARDUBICE
Series A
Faculty of Chemical Technology
2 (1996)

TERMINAL VELOCIY OF SPHERICAL PARTICLES FALLING THROUGH NON-NEWONIAN SUSPENSIONS

Ivan MACHAČ[a], Iva ULBRICHOVÁ[a], Tim P. ELSON[b], and David J. CHEESMAN[b]
[a]Department of Chemical Engineering, University of Pardubice
[b]Department of Chemical and Biochemical Engineering, University College London, London

Received May 10, 1995

The terminal falling velocities of glass, steel, and lead spheres in shear-thinning suspensions of kaolin and titanium dioxide in water solutions of glycerol have been measured. Overall, 130 spherical particle - suspension combinations have been tested giving a Reynolds number range of $0.001 < Re_{tn} < 452$.

The suitability of the correlations presented for the prediction of the drag coefficient of spheres falling through power-law and Herschel-Bulkley model fluids, has been evaluated by comparing their predictions with the above-mentioned experimental data.

Introduction

The fundamental hydrodynamic characteristics of the motion of a particle falling through a fluid are the drag coefficient c_D and terminal falling velocity u_t. Knowledge of these quantities is of a great theoretical and practical interest in both Newtonian and non-Newtonian fluids.

The prediction of c_D and u_t for rigid spheres falling through Newtonian fluids is already well-known and the correlations available can be used with sufficient accuracy over a wide range of conditions (e.g. Refs[1,2]). Over the last thirty years, considerable attention has also been paid to the investigation of the influence of non-Newtonian fluid behaviour on the motion of spheres. The results of previous theoretical and experimental studies on the flow of Newtonian and non-Newtonian fluids past a sphere have been reviewed for example by Chhabra[3].

Regarding the variety and complexity of non-Newtonian anomalies, no high degree of accuracy for the prediction of drag coefficients can be expected for a non-viscometric flow of a non-Newtonian fluid around a sphere. If a suitable predictive method for determination of c_D is to be selected, it is useful to lean upon experimental experience.

In our contribution, new measurements of the terminal settling velocity are presented extending the available experimental database on the fall of spherical particles through non-Newtonian suspensions. Also, in comparing the experimental and calculated values of the terminal falling velocity, the suitability of the equations proposed for the prediction of the drag coefficient is evaluated.

Drag Coefficient and Terminal Falling Velocity

The drag force acting on a sphere, diameter d, and density ρ_s, falling at velocity u through a fluid, density ρ, can be expressed as

$$F_D = c_D \frac{\pi d^2}{4} \frac{u^2}{2} \rho \tag{1}$$

For a sphere falling at its terminal velocity u_t, the drag force is balanced with the gravitational and buoyancy forces, so that

$$c_D = \frac{4}{3} g d \frac{(\rho_s - \rho)}{\rho u^2} \tag{2}$$

The terminal falling velocity u_t may be calculated from relationship (2) if the drag coefficient can be determined. For a sphere falling in an unbounded fluid, the drag coefficient depends on rheological behaviour of the fluid and on the flow regime.

Newtonian Fluids

For the motion of a solid sphere in a Newtonian fluid, the drag coefficient is a function of the particle Reynolds number

$$Re_t = \frac{du_t\rho}{\mu} \tag{3}$$

In the creeping flow region (Stokes region, $Re_t < 0.2 \sim 1$)

$$c_D = \frac{24}{Re_t} \tag{3}$$

For the transition flow region ($1 < Re_t < 1000$), empirical relationships have been suggested for expressing the drag coefficient. For example, Khan and Richardson[1] proposed the relationship

$$c_D = \left(2.25\,Re_t^{-0.31} + 0.36\,Re_t^{0.06}\right)^{3.45} \tag{5}$$

Other expressions for the spherical particle drag coefficient determination are presented in literature (e.g.[1,2,4]).

Purely Viscous Non-Newtonian Fluids

The common non-Newtonian anomaly of fluids with complex structure is the variation of their viscosity with shear rate $\dot{\gamma}$ (or shear stress τ). In the vast majority of cases, the viscosity decreases with increase in the shear rate (shear thinning behaviour, or pseudoplasticity). For time independent fluids, the viscosity function $\eta = \eta(\dot{\gamma})$ can be expressed by a flow model of generalized Newtonian fluid (e.g.[5]). The simplest (and the most frequently used in engineering applications) model is the "power law"

$$\frac{\tau}{\dot{\gamma}} \equiv \eta = K\dot{\gamma}^{n-1} \tag{6}$$

where K (fluid consistency) and n (flow behaviour index) are the experimental model parameters.

Theoretical treatments of the flow of purely viscous non- Newtonian fluids past a sphere have been restricted to creeping flow. For a power-law fluid, the drag coefficient can be expressed as

$$c_D = \frac{24}{Re_{tn}} X(n) \tag{7}$$

in this region.

Here $X(n)$ is the drag coefficient correction function which depends on the flow index n, and

$$Re_{tn} = \frac{d^n u_t^{2-n}\rho}{K} \tag{8}$$

is the particle Reynolds number modified for a power-law liquid. The

dependence $X = X(n)$ differs according to authors who solved the above mentioned flow problem[6-13].

The form of $X = X(n)$ given by some of above cited authors are shown in Fig. 1. It is clear from the wide variation in predicted values of X that no accurate prediction of drag correction function is easily available[11].

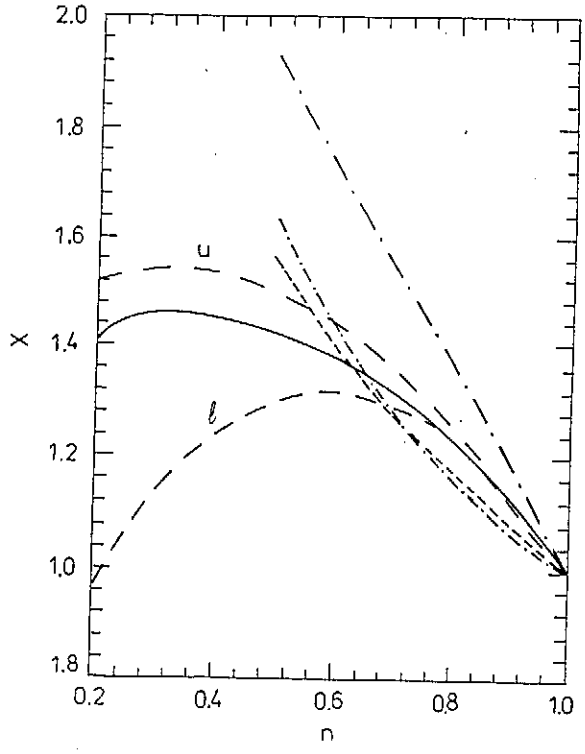

Fig. 1 Dependence of the correction function X upon power-law index: —·— Kawase and Ulbrecht[9], -·-·- Acharya et al.[8], - - - - - Kawase and Moo-Young[12], ——— Dazhi and Tanner[11], ——— Cho and Hartnett[10], u - upper bound, ℓ - lower bound

For the transition flow region ($1 < Re_{tn} < 1000$), empirical correlations have been proposed for coefficient c_D. For example, Acharya et al.[8] presented the relationship

$$c_D = \frac{24}{Re_{tn}} X(n) + \frac{F_1(n)}{Re_{tn}^{F_2(n)}} \quad , \tag{9}$$

where

$$X(n) = 3^{(3n-3)/2} \frac{33n^5 - 64n^4 - 11n^3 + 97n^2 + 16n}{4n^2(n+1)(n+2)(2n+1)} \tag{10}$$

$$F_1(n) = 10.5n - 3.5 \tag{11}$$

$$F_2(n) = 0.32n + 0.13 \tag{12}$$

The validity of Eq. (9) is limited by the conditions $0.5 \leq n \leq 1$, $Re_m \leq 1000$. The form of equation (10) has been corrected by Kawase and Ulbrecht[9] to

$$X(n) = 3^{(3n-3)/2} \frac{-22n^2 + 29n + 2}{n(n+2)(2n+1)} \tag{10a}$$

For $Re_{tn} > 1$, Lali et al.[14] suggested that the coefficient c_D can be determined using relations valid for Newtonian fluids if the Reynolds number Re_{tn} is substituted for Re_t. This possibility has been verified by Chhabra[15] for the fall of spheres through polymer solutions over the range of $0.535 \leq n \leq 1$ and $1 < Re_m < 1000$.

The concept of yield stress can be helpful in solving some practical flow situations of concentrated dispersed systems. The rheological behaviour of a Bingham plastic and a power-law fluid is combined in the Herschel-Bulkley flow model (e.g.[5])

$$\eta = \frac{\tau_y}{\dot{\gamma}} + K_p \dot{\gamma}^{n_p - 1} \tag{13}$$

with the parameters τ_y ("yield stress"), K_p and n_p. The fall of spheres through Bingham fluids ($n_p = 1$, $K_p = \mu_p$) was investigated by several authors[16-21].

Beris et al.[19] solved the creeping motion of a sphere using a finite-element method. Ito and Kajiuchi[18] applied the "similarity law of energy dissipation", and found that the drag coefficient can be determined from correlations valid for Newtonian fluids, if the generalized particle Reynolds number

$$Re_t^+ = Re_o[f(N_B) + 1]^{-1} \tag{14}$$

is substituted for Reynolds number Re_t.

Here $Re_o = (du_t\rho)/\mu_p$ is the particle Reynolds number defined for a Bingham fluid. The function $f(N_B)$ of the plasticity number

$$N_B = \frac{\tau_y d}{\mu_p u_t} \tag{15}$$

has to be determined experimentally.

For $f(N_B) = N_B$, the Reynolds number Re_t^+ becomes identical with the number Re_{tB}, where

$$Re_{tB} = \frac{d u_t \rho}{\mu_p + \tau_y \frac{d}{u_t}} = Re_o \frac{1}{1 + N_B} \tag{16}$$

The number Re_{tB} for a Bingham fluid is analogous to the number Re_{tn} for a power-law fluid. Both numbers result from the Newtonian fluid Reynolds number Re_t in which the non-Newtonian viscosity η, calculated from the corresponding viscosity models at the characteristic shear rate $\dot{\gamma} = u_t/d$, is substituted for the dynamic viscosity μ. If this method of Reynolds number Re_t modification is applied to a Herschel-Bulkley model fluid, then

$$Re_{tHB} = \frac{d^{n_p} u_t^{2-n_p} \rho}{\tau_y \left(\frac{d}{u_t}\right)^{n_p} + K_p} \tag{17}$$

Analogously to the sphere fall through a Bingham plastic fluid, it can be expected that the Reynolds number Re_{tHB} can be used for the prediction of the coefficient c_D of a sphere falling through Herschel-Bulkley model fluids from the relationships valid for Newtonian fluids.

Dedegil[20] recommended a similar way of prediction of the drag coefficient of a sphere falling through viscoplastic fluids. Unlike Eq. (2), he defined the sphere drag coefficient as

$$c_{DP} = \frac{2}{u_t^2 \rho}\left[\frac{2}{3}(\rho_s - \rho) g d - \pi \tau_y\right] \tag{18}$$

Evaluating the measurements of Valentik and Whitmore[16], he has stated that

$$\text{for } Re_{tB} < 8, \qquad c_{DP} = \frac{24}{Re_{tB}}, \tag{19}$$

$$\text{for } 8 \le Re_{tB} \le 150, \qquad c_{DP} = \frac{22}{Re_{tB}} + 0.25, \tag{20}$$

$$\text{for } Re_{tB} > 150, \qquad c_{DP} = 0.4. \tag{21}$$

Experimental

Terminal settling velocities were measured of spherical particles falling through suspensions of kaolin or titanium dioxide in water solutions of glycerol.

Two sets of experiments were made and are numbered (1) and (2) in the accompanying tables and figures.

The particles used were glass, lead, and steel spheres. Their characteristics are given in Table I. The suspensions were prepared by gradual dispersion of

powdered kaolin KKN or titanium white RD-54 into water solutions of glycerol. The dispersion of solid was achieved using the mixer Etamira (6000 rpm) in the first set of experiments[22] and using the turbine impeller (2000 rpm) in the second. The shear stress-shear rate dependences of the suspensions were measured using rotary cylindrical rheometers Rheotest II (first set of experiments) and Rheomat 30 (second set). Examples of suspension flow curves

Table I Characteristics of the particle used

Sphere symbol	Diameter $m \times 10^{-3}$	Density kg m^{-3}	Sphere symbol	Diameter $m \times 10^{-3}$	Density kg m^{-3}
K1	2.782	2504	K10	11.084	7842
K2	3.457	2867	K11	12.681	7840
K3	4.117	2596	K12	14.265	7836
K4	3.163	7834	K13	15.041	7830
K5	3.953	7826	K14	15.839	7829
K6	4.731	7830	K15	1.973	11093
K7	5.975	7861	K16	2.291	11260
K8	7.893	7856	K17	2.851	11195
K9	9.503	7852	K18	3.902	11157

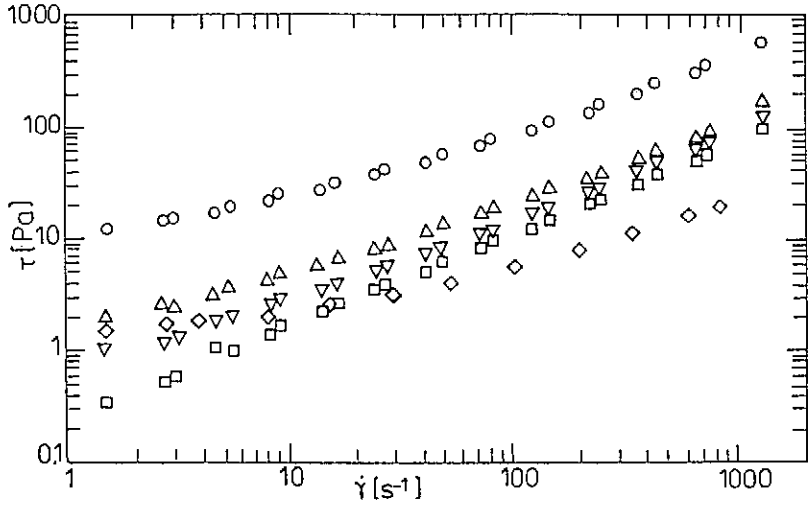

Fig. 2 Typical flow curves for the suspension tested: ○ - 15% kaolin (1), △ - 10% kaolin (1), □ - 6% kaolin (1), ▽ - 35% TiO_2, 60% glycerol (1), ◇ - 30% TiO_2 (2)

are shown in Fig. 2. The data were fitted to the power-law and Herschel-Bulkley flow models. Since the power law-model fits suspension viscometric data with sufficient accuracy over a limited interval only, the parameters K and n were determined in the shear rate range downward from the level of shear rate specified by maximum value of $\dot{\gamma} = u_t/d$ which is considered to be relevant in the flow around the falling sphere. Parameters τ_y, K_p, and n_p of the Herschel-Bulkley model were determined making use of the all viscometric data available. The parameters obtained for the test suspensions are given in Table II. Rather different values of flow model parameters for the kaolin suspensions of equal concentration investigated in both sets of experiments show the influence of the method of solid dispersion on rheological properties of the suspensions.

Table II Parameters of the power-law and Herschel-Bulkley models

Suspensions	Set of experiments	Power-law			Herschel-Bulkley model		
		n	K Pa s^n	$\dot{\gamma}_{max}$ s^{-1}	τ_y Pa	n_p	K_p Pa s^n
6% wt. kaolin in	1.	0.762	0.336	146	0.032	0.799	0.297
80% glycerol	2.	0.720	0.564	147	0.063	0.765	0.481
8% wt. kaolin in	1.	0.629	0.816	146	0.840	0.781	0.402
80% glycerol	2.	0.614	1.342	147	0.148	0.668	1.153
10% wt. kaolin in	1.	0.566	1.319	146	1.226	0.745	0.590
80% glycerol	2.	0.570	1.921	147	0.172	0.615	1.704
15% wt. kaolin in	1.	0.378	6.592	146	7.870	0.703	1.326
80% glycerol	2.	0.349	10.80	108	1.003	0.392	9.361
30% wt. TiO_2 in	1.	0.737	0.353	146	0.337	0.865	0.199
80% glycerol	2.	-	-	-	-	-	-
30% wt. TiO_2 in	1.	-	-	-	-	-	-
40% glycerol	2.	0.250	1.325	158	0.381	0.414	0.704
35% wt. TiO_2 in	1.	0.673	0.615	146	0.565	0.809	0.338
80% glycerol	2.	-	-	-	-	-	-
35% wt. TiO_2 in	1.	0.424	0.717	146	0.924	0.742	0.150
60% glycerol	2.	-	-	-	-	-	-

Two different methods were used for indication of the position of a particle falling through a suspension filled in the test Perspex cylindrical columns. In the first set of experiments with the steel balls K4-K14, the time was registered of the particle passage between two electromagnetic coils mounted on the column of 4 cm in diameter in the distance of 0.5 m. The stop watch reading to 0.01 s was used for timing the balls. The timing was repeated 30 times for each individual sphere. The terminal falling velocity was

determined as a ratio of the pass distance and the average falling time. In the second set of experiments with glass, steel (K4-K6), and lead balls, the X-ray equipment in a cineradiography arrangement was used for monitoring the motion of particles[23]. The time of a particle fall along the path of 0.1 m through a liquid filled in the column of 7 cm in diameter was determined analyzing the video-tape record using an editing video player. The automatic frame count recorded on the tape allowed a resolution of 0.02 s.

Overall, 130 particle-suspension combinations were tested giving a Reynolds number range of $0.001 < Re_{tn} < 452$.

Results and Discussion

Experimental results of sphere drop tests are usually displayed in a form of a drag coefficient plotted against the Reynolds number. For this purpose, the values of the drag coefficients c_D and c_{DP} were calculated according to Eqs (2) and (18), respectively, making use of the experimental data of the terminal falling velocities which had first been corrected for the wall effect[22]. Here the suspensions were regarded as inelastic power-law fluids and the values of wall correction factor, defined as the ratio of the terminal velocity of a sphere in a bounded medium to that in an unbounded one, were determined according to the relationships given by Faxen[24] in the creeping flow region or by Chhabra and Uhlherr[25] in the transition flow region. The suitability of that correction was verified by measuring the terminal velocities of steel spheres K4-K8 in two different columns of 2 cm and 4 cm in diameters. The mean deviation between corresponding corrected values of terminal falling velocities evaluated from measurements in both columns was 6 %, the maximum deviation was 11 %. An example of terminal velocity data u_{t2} and u_{t4}, obtained from measurements in the above-mentioned test columns, along with the corresponding corrected terminal velocity data $u_{t2,\infty}$ and $u_{t4,\infty}$ is shown in Table III for suspensions of 15% kaolin in 80% glycerol, and 35% TiO_2 in 60% glycerol. In this table, the individual deviations between values $u_{t2,\infty}$ and $u_{t4,\infty}$ are given as well.

Then, the dependences $c_D = c_D(Re_{tn})$, $c_D = c_D(Re_{tHB})$, and $c_{DP} = c_{DP}(Re_{tHB})$ were plotted. The obtained dependences c_D vs. Re_{tn} and c_{DP} vs. Re_{tHB} are shown, along with the Newtonian drag curves (Eq. (5)) and the Bingham fluid drag curve (Eqs (19) - (21)), in Fig. 3. It can be seen that the form of these experimental dependences do not markedly differ from each other. The experimental points measured by the two different techniques in the two sets of experiments coincide and follow the course of the standard Newtonian drag coefficient curve. However, it must be observed that the portraying the experimental results in the way used in Fig. 3 may be misleading in the case of highly shear thinning non-Newtonian systems, especially at low Reynolds numbers[26].

Therefore, to evaluate the suitability of the drag coefficient relationships

Table III Terminal velocity data measured in columns of 2 and 4 cm diameter

	Particle	u_{t2} m s^{-1}	u_{t4} m s^{-1}	$u_{t2,\infty}$ m s^{-1}	$u_{t4,\infty}$ m s^{-1}	Deviation %
15% wt. kaolin in 80% glycerol (1)	K4	0.017	0.020	0.026	0.024	6.5
	K5	0.026	0.037	0.044	0.047	-6.0
	K6	0.044	0.065	0.084	0.086	-2.2
	K7	0.078	0.109	0.142	0.131	8.4
	K8	0.110	0.212	0.265	0.263	1.0
35% wt. TiO_2 in 60% glycerol (1)	K4	0.239	0.237	0.252	0.242	3.9
	K5	0.319	0.333	0.337	0.340	-0.8
	K6	0.400	0.423	0.427	0.431	-1.0
	K7	0.502	0.557	0.550	0.568	-3.3
	K8	0.605	0.735	0.727	0.755	-3.8

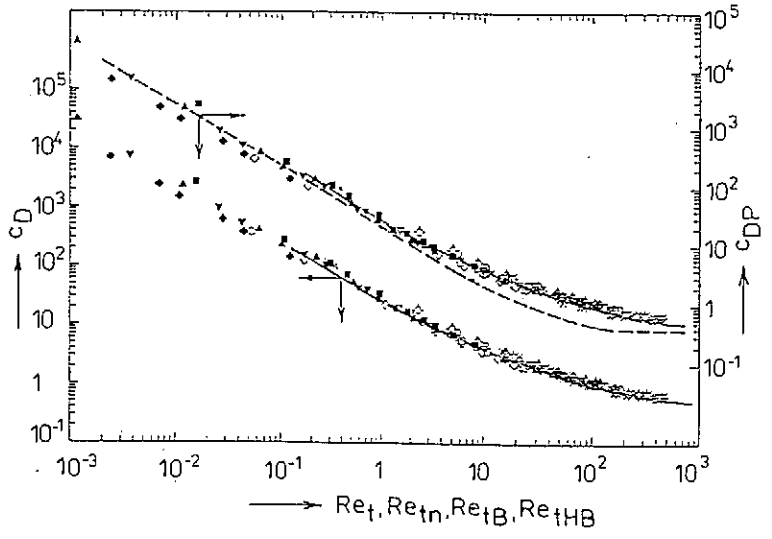

Fig. 3 Experimental variation of the sphere drag coefficients with Reynolds numbers: □, ■ - 6% kaolin (1), (2); △, ▲ - 8% kaolin (1), (2); ▽, ▼ - 10% kaolin (1), (2); ◇, ◆ - 15% kaolin (1), (2); ○ - 30% TiO_2 (1); ☼ - 35% TiO_2, 80% glycerol (1); × - 30% TiO_2 (2); ☼ - 35% TiO_2, 60% glycerol (1); ——— Eq. (5); — — — Eqs (19) - (21)

available for the prediction of the terminal falling velocity of a sphere moving in a shear thinning suspension, the experimental data u_{te} were compared with calculated data u_{tc} of terminal falling velocities. Values of u_{tc} were calculated

by an iterative method from Eqs (2) and (18) into which the different values of the drag coefficient, determined according to relationships tested, were substituted.

The power-law (6) and Herschel-Bulkley model (13) were applied to obtain an approximation of suspension viscosity. In the creeping flow region, the values of c_D were determined from equation (7) using the correction factor $X(n)$ expressed by Eq. (10) (for $n > 0.5$ only), and making use of the arithmetic mean of the upper and lower bounds on the drag correction factor given by Cho and Hartnett (Fig. 1). The values of the drag coefficient c_{DP} were determined according to Eq. (19).

In the transition flow region, Eqs (9) and (5) were tested for power-law fluids. In the later case, the Reynolds number Re_{tn} was substituted for Re_t. For Herschel-Bulkley model fluids, the terminal falling velocities u_{tc} were calculated using both Eqs (2) and (18), the drag coefficient was determined according to Eq. (5) or Eqs (19) - (21) substituting the number Re_{tHB} for Re_t in this case.

The agreement between individual values of u_{te} and u_{tc} was evaluated according to the relative deviations

$$\delta_i = \frac{(u_{tc} - u_{te})}{u_{te}} 100 \quad \%, \tag{22}$$

and for individual sets of measurements in suspensions investigated according to the mean relative deviations

$$\bar{\delta} = \frac{1}{N} \sum_{i=1}^{N} |\delta_i| \tag{23}$$

For creeping flow conditions, the discrepancy between experimental and calculated terminal velocity data is evident from Fig. 4. It follows from the results obtained that only the suspension of TiO_2 and the 6% and 8% kaolin suspensions can be treated as power law fluids if a sphere terminal falling velocity is estimated using Eq. (2) along with Eq. (7). In this case, the deviations $\bar{\delta}$ do not exceed the value 30%. At the same time, the factor $X(n)$ given by Eq. (10) is recommended to be used only for suspensions characterized by the flow index $n > 0.65$. For more concentrated suspensions of kaolin in glycerol, the power law does not apparently represent well their more complex rheological properties. In the case of 10% kaolin suspension, which is in respect of its value of τ_y (Tab. II) more plastic than the kaolin suspensions with lower concentration, good results of terminal falling velocity prediction were obtained making use of Eqs (18) and (19) substituting the Reynolds number Re_{tHB} for Re_{tB}. For 15% kaolin suspension, which shows an evident thixotropic behaviour as well, the prediction of terminal falling velocities fails in all the methods tested. In this case, the value of a sphere terminal velocity strongly depended on the time of suspension structure recovery after its pouring into test column. An

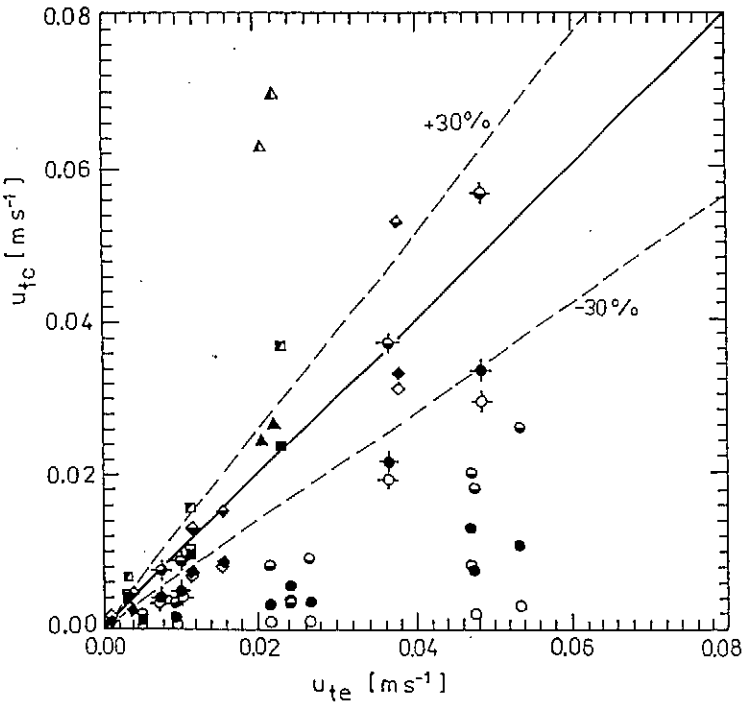

Fig. 4 Comparison of the experimental terminal falling velocity data obtained in creeping flow region with those predicted using Eq. 7 (solid symbols - $X(n)$ from Eq. (10), open symbols - $X(n)$ according to Cho and Hartnett[10]) and using Eq. (19) (half solid symbols): □, ■, ◩ - 6% kaolin (2); ◇, ◆, ◈ - 8% kaolin (2); ⟡, ✦, ✧ - 10% kaolin (2); ○, ●, ◒ - 15% kaolin (1), (2); ▲, △ - 30% TiO_2 (2)

example of the dependences of the terminal falling velocity u_t upon the suspension recovery time t_R is shown in Fig. 5 for the steel sphere K5 falling through different test suspensions. The ratio of the value u_t measured immediately after pouring the test suspension into Perspex column to the final, steady-state value of u_t is 1.03, 1.10, and 1.46 for 6, 10, and 15% kaolin suspensions, respectively. At the same time, a significant influence of kaolin sedimentation on the value of u_t has been excluded by measurements of electrical conductivity of 15% kaolin suspension at different levels of test column over several hours.

For transition flow conditions ($Re_{tn} > 1$), the deviations $\bar{\delta}$ are summarized in Table IV. If Eq. (2) is used along with Eqs (9) - (12) for the u_{tc} calculations, acceptable deviations $\bar{\delta}$ up to 30% (column 3 in Table IV) are obtained only for suspensions with the flow index $n > 0.6$. Surprisingly good agreement between the experimental and calculated terminal falling velocity data is achieved when determining the sphere drag coefficient according to Eq. (5) substituting both the Reynolds number Re_{tn} and Re_{tHB}. When the power

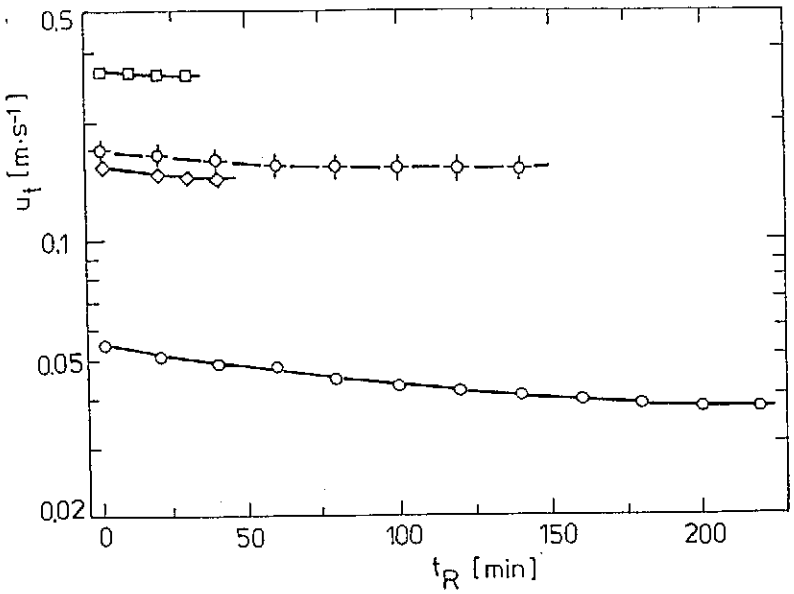

Fig. 5 Dependence of the terminal falling velocity upon the time of measurement: □ - 6% kaolin (1); -◇- 10% kaolin (1); ○ - 15% kaolin (1); ◇ - 35% TiO_2, 80% glycerol

law is applied, the deviation for the whole set of terminal falling velocity data is 9.3% (column 4 in Table IV). The calculation based on the Reynolds number Re_{tIIB} yields somewhat lower deviations $\bar{\delta}$ (columns 5 and 6 in Table IV). The comparison of experimental terminal velocity data with those calculated according to Eqs (2) and (5) substituting Reynolds number Re_{tIIB} for Re_t is shown in Fig. 6. With respect to the relatively low values of the "yield stress" parameter τ_y of the test suspensions (Table II), the difference between the values of u_{tc} calculated using both Eq. (2) and Eq. (18) is not significant, except the suspension of 15% kaolin. For this suspension, the more accurate prediction of u_t was obtained using Eq. (2).

In the transition flow region, our experiments are in accordance with the results obtained by Briscoe et al.[21] for the fall of smooth spheres in the power law or Bingham plastic water suspensions of bentonite. On the other hand, it is evident from Fig. 3 that the data of c_{DP} calculated according to Eqs (19) - (21) do not correspond to our experiments in this flow region. The deviations δ of experimental and calculated terminal velocity data range from 13% to 94% in this case, the deviation for the whole set of data being 65.8% (column 7 in Table IV). It is necessary to note that the Dedegil's evaluation of experimental data of Valentik and Whitmore[16] resulting in Eqs (19) - (21) may be strongly distorted by the way of interpretation of shear stress-shear rate data. Those data are presented by Valentik and Whitmore only in a graphical form and are not sufficiently detailed, especially at the relevant low values of shear rates ($\dot{\gamma} < 100$).

Table IV Deviations $\bar{\delta}$ for test suspensions, $Re > 1$

Suspension	Set of experiments	$\bar{\delta}$, %				
		Eq. (2)			Eq. (18)	
		c_D from Eq. (9)	c_D from Eq. (5) with Re_{in}	c_D from Eq. (5) with Re_{tHB}	c_{DP} from Eq. (5) with Re_{tHB}	c_{DP} from Eqs (19) - (21) with Re_{tHB}
6% wt. kaolin in 80% glycerol	1.	10.7	4.0	4.2	2.8	62.9
	2.	10.3	10.0	8.7	8.5	57.0
8% wt. kaolin in 80% glycerol	1.	11.8	2.1	2.4	1.9	69.8
	2.	32.5	6.8	10.0	10.8	24.2
10% wt. kaolin in 80% glycerol	1.	19.6	3.8	3.7	4.4	65.3
	2.	44.2	10.0	12.8	13.0	13.1
15% wt. kaolin in 80% glycerol	1.	(50.4)*	18.6	7.5	19.5	55.1
	2.	-	-	-	-	-
30% wt. TiO_2 in 80% glycerol	1.	8.2	12.5	7.9	6.6	72.3
	2.	-	-	-	-	-
30% wt. TiO_2 in 40% glycerol	1.	-	-	-	-	-
	2.	-	14.7	10.0	9.9	93.9
35% wt. TiO_2 in 80% glycerol	1.	9.1	17.9	18.0	14.7	92.0
	2.	-	-	-	-	-
35% wt. TiO_2 in 60% glycerol	1.	(30.9)*	5.5	4.8	3.9	52.0
	2.	-	-	-	-	-
All data		13.8	9.3	7.7	8.0	65.8

* outside the range of validity

Conclusion

The prediction of terminal falling velocity has been investigated for spheres moving in shear-thinning suspensions.

It follows from the results obtained in creeping flow region that among the suspensions tested only the suspensions of 6% and 8% kaolin, and

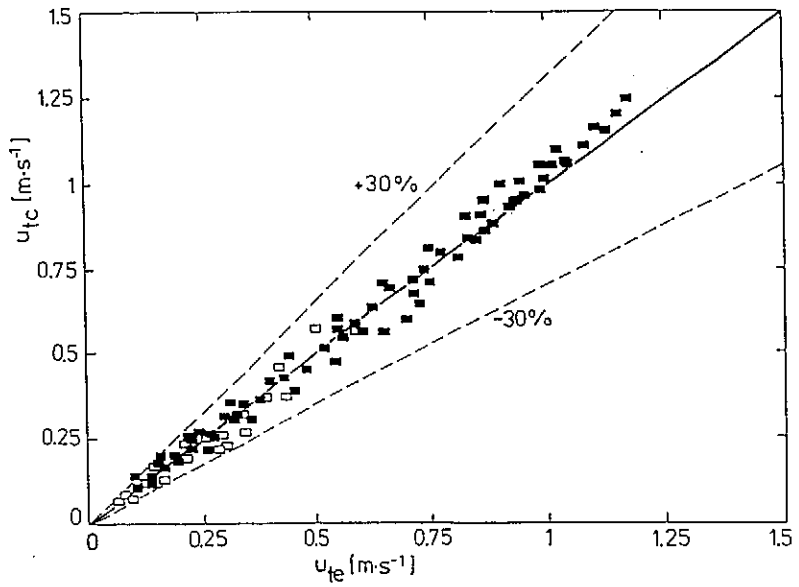

Fig. 6 Comparison of the experimental terminal falling velicity data obtained in transition flow region with those predicted according to Eqs (2) and (5) substituting Re_{tHB} for Re_t ■ - set (1); □ - set (2)

suspension of titanium dioxide can be treated as power-law fluids if a sphere terminal falling velocity is calculated. For the more concentrated kaolin suspensions, the power law does not apparently represent well their more complex rheological behaviour. To obtain a more reliable basis for the terminal falling velocity estimation in this flow region, further investigations are needed.

The results obtained in transition flow region confirmed that the unified approach, discussed by Chhabra[15] for polymer solutions, may also be successfully applied to prediction of the terminal falling velocity of a sphere moving in shear thinning suspensions. For the suspensions tested, a rather more accurate estimation of u_t was achieved if the Herschel-Bulkley model was used instead of the power-law for approximation of the viscosity function of a suspension.

Symbols

c_D	sphere drag coefficient expressed by Eq. (2)
c_{DP}	sphere drag coefficient expressed by Eq. (18)
d	particle diameter, m
F_D	drag force, N
$F_1(n)$	flow index function expressed by Eq. (11)
$F_2(n)$	flow index function expressed by Eq. (12)

g	gravitational acceleration, m s^{-1}
K	power law model parameter (fluid consistency), Pa s^n
K_p	Herschel-Bulkley model parameter, Pa s^n
N_B	plasticity number defined by Eq. (15)
n	power-law model parameter (flow behaviour index)
n_p	Herschel-Bulkley model parameter
Re_o	particle Reynolds number defined for a Bingham fluid
Re_t	particle Reynolds number for a Newtonian fluid defined by Eq. (3)
Re_t^*	generalized Reynolds number defined for a Bingham fluid by Eq. (14)
Re_{tB}	particle Reynolds number defined for a Bingham fluid by Eq. (16)
Re_{tn}	particle Reynolds number defined for a power-law fluid by Eq. (8)
Re_{tHB}	particle Reynolds number defined for a Herschel-Bulkley model fluid by Eq. (17)
t_R	suspension structure recovery time, s
u	fluid velocity, m s^{-1}
u_t	particle terminal falling velocity, m s^{-1}
$X(n)$	drag coefficient correction function
$\dot{\gamma}$	shear rate, s^{-1}
$\underline{\delta}_i$	relative deviation expressed by Eq. (22)
δ	mean relative deviation expressed by Eq. (23)
η	fluid non-Newtonian viscosity, Pa s
μ	fluid dynamic viscosity, Pa s
μ_P	Bingham model parameter (plastic viscosity), Pa s
ρ	fluid density, kg m^{-3}
ρ_s	particle density, kg m^{-3}
τ	shear stress, Pa
τ_y	Herschel-Bulkley model parameter ("yield stress"), Pa

Indexes

c	calculated
e	experimental
∞	unbounded fluid

References

1. Khan A.R., Richardson J.F.: Chem. Eng. Commun. **62**, 135 (1987).
2. Hartman M., Yates J.G.: Collect. Czech. Chem. Commun. **58**, 961 (1993).
3. Chhabra R.P.: Bubbles, *Drops, and Particles in Non-Newtonian Fluids*, CRC Press Boca Raton, FL. 1993.
4. Chhabra R.P.: Journal de Recherches Hydrauliques **25**, 216 (1986).

5. Tanner R.J.: *Engineering Rheology*, Oxford University Press, New York 1985.
6. Tomita Y.: Bull. J.S.M.E. 2, 469 (1959).
7. Wasserman M.L., Slattery J.C.: AICHE J. **10**, 383 (1964).
8. Acharya A., Mashelkar R.A., Ulbrecht J.: Rheol. Acta, **15**, 454 (1976).
9. Kawase Y., Ulbrecht J.J.: Chem. Eng. Commun. **8**, 213 (1981).
10. Cho Y.I., Hartnett J.C.: J. Non-Newt. Fluid Mech. **12**, 243 (1983).
11. Dazhi G., Tanner R.I.: J. Non-Newt. Fluid Mech. **17**, 1 (1985).
12. Kawase Y., Moo-Young M.: J. Non-Newt. Fluid Mech. **21**, 167 (1986).
13. Tripathi A., Chhabra R.P., Sundararajan T.: Ind. Eng. Chem. Res. **33**, 403 (1994).
14. Lali A.M., Khare A.S., Joshi J.B., Migam K.D.P.: Powder Technol. **57**, 47 (1989).
15. Chhabra R.P.: Chem. Eng. Process **28**, 89 (1990).
16. Valentik L., Whitmore R.L.: Brit. J. Appl. Phys. **16**, 1197 (1965).
17. Ausley R.W., Smith T.N.: AICHE J. **13**, 1193 (1967).
18. Ito S., Kajiuchi T.: J. Chem. Eng. Jap. **2**, 19 (1969).
19. Beris A.N., Tsamopoulos J.A., Armstrong R.C., Brown R.A.,: J. Fluid Mech. **158**, 219 (1985).
20. Dedegil M.Y.: J. Fluid Eng. **109**, 319 (1987).
21. Briscoe B.J., Luckham P.F., Ren S.R.: Powder Technology **76**, 165 (1993).
22. Hladík T.: *Fall of spherical particle through non-Newtonian suspensions (in Czech)*, Diploma Thesis, VŠCHT Pardubice 1992.
23. Elson T.P.: Chem. Eng. Commun. **94**, 143 (1990).
24. Happel J., Brenner H.: *Low Reynolds number hydrodynamics*, Prentice-Hall, Inc., Englewood Cliffs, N. J. 1965.
25. Chhabra R.P., Uhlherr P.H.T.: Chem. Eng. Commun. **5**, 115 (1980).
26. Sheffield R.E., Metzner A.B.: AICHE J. **22**, 736 (1976).